



## The influence of boron impurity for the adiabatic charging energies of thiol-ended thiophene: A DFT study

Seval Çapanlar<sup>a</sup> and Ali Kemal Garip<sup>\*b</sup>

<sup>a</sup>Department of Chemistry, <sup>b</sup>Department of Physics, Zonguldak Bulent Ecevit University, Zonguldak, Turkey

E-mail: akemal.garip@beun.edu.tr

Manuscript received online 30 December 2019, revised 24 February 2020, accepted 26 February 2020

In this study, the charging energies of both modified and pure thiol-ended thiophene molecule were calculated with the quantum-chemical methods. The geometry optimizations of the molecules in gas phase have been performed for different charge states (+1, 0, -1) of the different boron impurity orientations at DFT level. The adiabatic ionization energy and adiabatic electron affinity of the thiol-ended thiophene molecule with four boron impurity derivatives were calculated using B3LYP/6-31G(d,p)++ basis set. The influence of the boron impurity has been investigated to control and adjust the HOMO-LUMO gap of the molecules. The calculated addition energies were compared and some of characteristic ones were depicted with the electrostatic maps. The molecule which has geminal boron atoms onto the sulphur has the largest addition energy and a larger HOMO-LUMO gap than the other thiol-ended thiophene molecule derivatives. This molecule with the largest addition energy in comparison with the others is the most possible candidate for MSET application with a good performance. As a consequence, both increased and decreased addition energies were obtained due to the number and orientation of the boron impurities in the thiol-ended thiophene molecule.

Keywords: Thiol-ended thiophene, boron impurity, charging energy, HOMO-LUMO gap.

### Introduction

In recent years, the usage of organic molecules in nanoelectronics as an active component takes lots of attention to improve the switching properties of Single Electron Transistors (SET)<sup>1</sup>. The conductance gap in the SET is relevant with the ionization energy and electron affinity of the molecule used as an island or semi-conductor quantum dot. The charging energies and electron transport properties of a molecular single-electron transistor (MSET) can be adjusted by modifying the molecule used as a component of the SET<sup>2</sup>.

In consideration of recent advances and researchs, the design of the organic molecules as transistor components is gaining much interest<sup>3-6</sup>. The charging energies of the anthracene molecule have been calculated by Srivastava *et al.* in isolated as well as in SET environments. They compared the switching speeds of anthracene SET and the other acene series SETs. The anthracene SET proposed in the study showed a good switching speed<sup>7</sup>. In order to control the conductance properties of the organic molecules, a useful choice is to substitute the carbon atoms with boron<sup>8,9</sup>. The boron and nitrogen impurity added benzene based single-electron

transistor (SET) were analyzed by Srivastava *et al.* either by replacing the last carbon atom or last hydrogen in the benzene. They concluded that the impurity added benzene show good improvement in the conductance in comparison to benzene based SET in terms of gate and source-drain bias<sup>10</sup>. Santhi Bhushan *et al.* studied the impact of boron substitution on anthracene island in order to model a better organic molecular SET. The proposed (10-boranyl anthracene-9-yl) borane SET was found to possess high switching speed and power efficiency than the other reported organic molecular SETs of its kind<sup>11</sup>. The influence of boron substitution in place of selected carbon atoms of pentane/pyridine molecules in isolated as well as in SET environments were studied by Srivastava *et al.* using the DFT-based *ab initio* methods. They have concluded that boron substitution to the island molecules plays an important role in the overall conductance and hence performance of the SET<sup>12</sup>.

Anu *et al.* studied both isolated and the SET configuration of thiol-ended thiophene molecule i.e. a thiophene molecule which the two dangling hydrogen atoms are substituted with sulphur atoms. Both thiol-ended thiophene molecule and

its chromium complex have been analyzed by Anu *et al.* for the charge stability and conductance dependence on the gate voltage and source-drain bias. The analysis showed that a remarkably improved conductance for the chromium complex of thiol-ended thiophene molecule than the pure thiol-ended thiophene molecule in the SET environment resulting in a fast switching metal-organic SET<sup>13</sup>.

To design the nanoelectronic devices such as SET, it is important to understand the individual properties of the molecules used as a transistor component. The quantum-chemical calculations are useful tools for design and characterization of the transport properties of charge carriers of organic semiconductors<sup>14</sup>. In the use of an organic molecule as a transistor component, determining the conditions for electronic transport in a SET is indispensable for the design of MSET. The electronic transport in a MSET is only possible when an electron can be moved from the highest occupied molecular orbital (HOMO) level to the lowest unoccupied molecular orbital (LUMO) level<sup>15</sup>. The addition energy which is the minimum energy required for this transition can be modified by manipulating the molecule used in SET. The present study deals with the improvement of the conductance properties of thiol-ended thiophene molecule as a quantum dot. Some modifications were performed on thiol-ended thiophene by substituting the carbon atoms with boron which has one valence electron less than a carbon. The charging energies of thiol-ended thiophene molecule with its modified derivatives have been theoretically investigated at DFT level.

#### Simulation method:

Density Functional Theory (DFT) calculations in this study were performed using GAMESS-US<sup>16</sup> program with the unrestricted Hartree-Fock (UHF) type of wavefunctions. The ground electronic state DFT optimizations were carried out using B3LYP/6-31G(d,p)++ level of basis set. The electronic properties such as ionization potentials, electronic states and energy gaps have been calculated successfully using the hybrid functional B3LYP in the previous studies<sup>17-21</sup>. The excited state energies in this study were also calculated with the same basis set.

The geometry optimizations have been performed for different charge states (+1, 0, -1) of the different impurity ratio in the gas phase. The calculated total energies have been used to define the charging energies, i.e. adiabatic ionization energy ( $E_I$ ) and adiabatic electron affinity ( $E_A$ ) of the

molecules, as

$$E_I = E^{+1} - E^0 \quad (1)$$

$$E_A = E^0 - E^{-1} \quad (2)$$

where  $E^0$  is the total energy of optimized neutral molecule,  $E^{+1}$  is the total energy of optimized positive charged molecule, and  $E^{-1}$  is the total energy of optimized negative charged molecule. The addition energy  $E_{\text{add}}$ , i.e. the energy required for adding an electron to a quantum dot, is given by eq. (3).

$$E_{\text{add}} = E_I - E_A \quad (3)$$

The Avogadro program was used as a molecular builder and visualization tool<sup>22</sup>.

## Results and discussion

DFT relaxation calculations in this study were performed for six different molecules in B3LYP/6-31G(d,p)++ level. The atomic arrangement of optimized ground state structures (neutral) are illustrated in Fig. 1. The HOMO-LUMO energy gap ( $\Delta_{\text{(H-L)}}$ ) is defined as the difference between the highest occupied molecular orbital energy and the lowest unoccupied molecular orbital energy. The  $\Delta_{\text{(H-L)}}$  is an indicator of chemical reactivity that we used it to compare the reactivities for investigated structures. The calculated energies with optimizations for different charge states (+1, 0, -1) are given in Table 1. The adiabatic ionization energy and adiabatic electron affinity of the molecules are also given in the same Table. The results associated with the  $\Delta_{\text{(H-L)}}$  and calculated addition energies are given in Table 2.

To test the reliability of the results in this study, we calculated the adiabatic ionization energy and adiabatic electron affinity of benzene molecule at DFT level. The literature value of ionization energy of benzene molecule is 9.245 eV<sup>23</sup>. The adiabatic electron affinity of benzene was found as

**Table 1.** Total energy calculation results

Molecule	$E^{+1}$ (a.u.)	$E^0$ (a.u.)	$E^{-1}$ (a.u.)	$E_I$ (eV)	$E_A$ (eV)
(I)	-1347.58	-1347.90	-1347.99	8.61	2.59
(II)	-1334.37	-1334.68	-1334.81	8.59	3.41
(III)	-1321.13	-1321.47	-1321.52	9.14	1.30
(IV)	-1334.30	-1334.61	-1334.75	8.51	3.72
(V)	-1321.01	-1321.34	-1321.41	9.02	1.84
(VI)	-231.78	-232.11	-232.09	8.97	-0.68

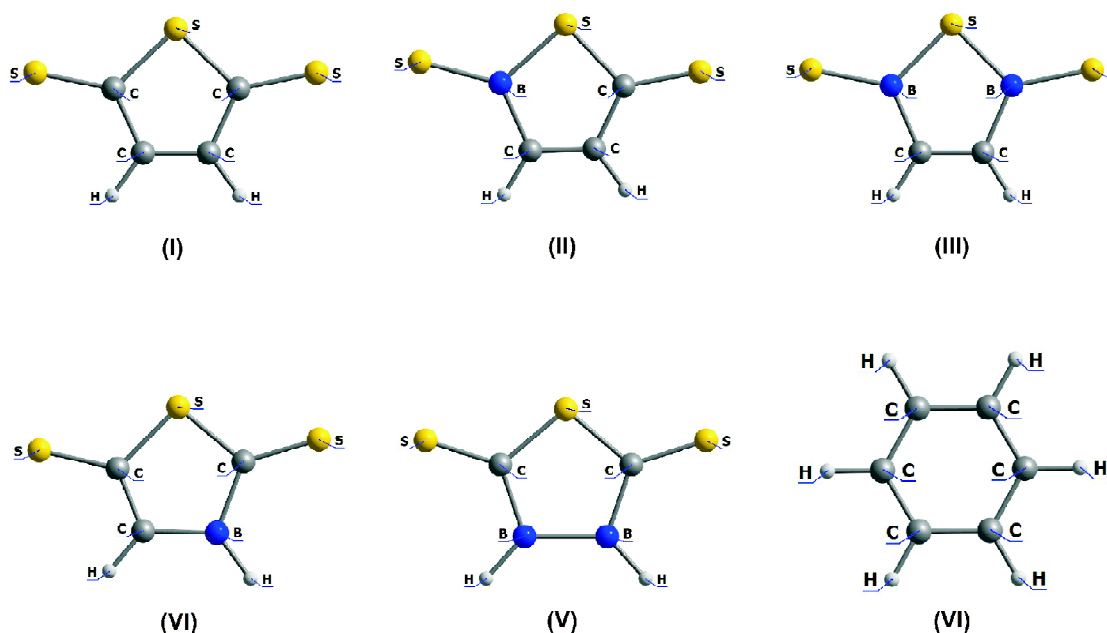


Fig. 1. The molecular labels and boron impurity orientations.

Table 2. The HOMO-LUMO energy gaps and addition energies		
Molecule lable	$\Delta_{(H-L)}$ (eV)	$E_{add}$ (eV)
(I)	-2.53	6.02
(II)	-3.12	5.18
(III)	-4.23	7.84
(IV)	-2.66	4.80
(V)	-1.25	7.19
(VI)	-6.60	9.65

$-0.70 \pm 0.14$  eV experimentally<sup>24</sup>, relatively good agreement with the theoretical result obtained in this study.

The simulation results showed that the molecule (III) has a larger  $\Delta_{(H-L)}$  than the other thiol-ended thiophene molecule derivatives, means less reactivity. The charge distributions of molecule (I), (III) and (IV) are depicted with the electrostatic potential maps in Fig. 2. The variation of electron densities were interpreted from the electrostatic surfaces. While the red colour electrostatic surfaces in Fig. 2 indicates the high electron density, the blue colour represents the low electron density. The molecule (III) has the maximum addition energy as impurity added thiol-ended thiophene, on the other hand the molecule (IV) has the minimum addition energy value. The molecule (I) which represents the thiol-ended thiophene has an intermediate addition energy without any

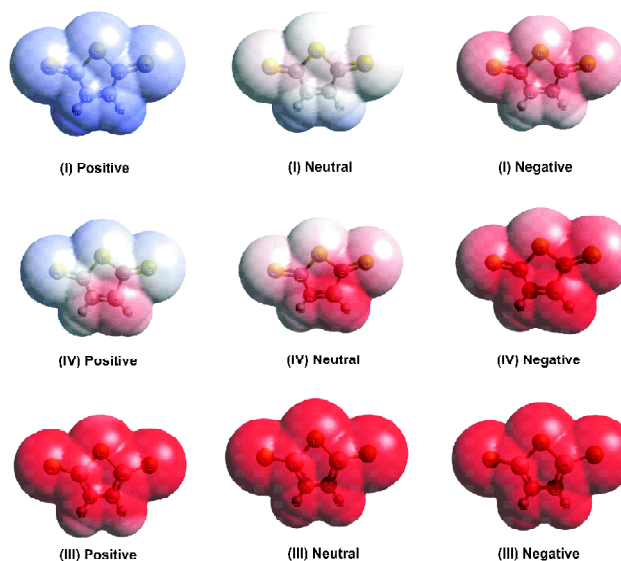


Fig. 2. Electrostatic potential maps of molecule (I), (IV) and (III).

boron impurity. In order to prevent the thermally induced random tunneling events, the most digital single-electron devices need higher values of addition energy. So, the larger addition energy can guarantee the operation ability. For the room temperature operation, the electron addition energy has to be as large as a few electron-volts<sup>25</sup>. In order to meet this

requirement, the size of the quantum dot has also to be less than  $\sim 1$  nm.

The molecule (III) which has geminal boron atoms onto the sulphur has the largest addition energy and a larger HOMO-LUMO gap than the other thiol-ended thiophene molecule derivatives. Accordingly, a further investigation is required to obtain the current vs voltage curve for promising new MSET in terms of the charge stability diagram for different gate and source/drain bias<sup>26</sup>.

The transport properties are highly affected by the small variations of the quantum dot size and shape. So, the Root Mean Square of Displacements (RMSD) for the molecule (I),

Molecule label	RMSD between $E^{+1}$ and $E^0$ (Å)	RMSD between $E^{-1}$ and $E^0$ (Å)
(I)	0.0497	0.0387
(III)	0.0559	0.0486
(IV)	0.0626	0.0340

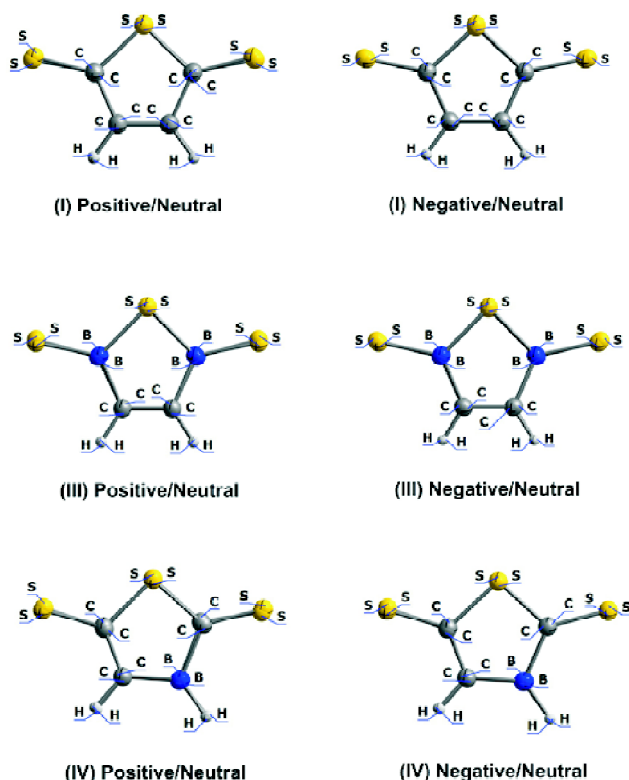


**Fig. 3.** The comparison of the optimized neutral and charged molecules (I, III and IV).

(III) and (IV) were also calculated between charged optimized molecules and neutral optimized molecules. The results are given in Table 3. The comparison of the optimized neutral and charged molecules (I), (III) and (IV) are depicted in Fig. 3. The optimized charged and neutral molecules have slightly different molecular geometries as seen in Table 3 and Fig. 3.

## Conclusions

The present work discusses the influence of boron impurity on the addition energy variation of thiol-ended thiophene molecule. The electron affinity and ionization energies can be controlled by different boron impurity variations for thiol-ended thiophene molecule.

In our findings, the molecule which has geminal boron atoms onto the sulphur has a larger HOMO-LUMO gap than the other thiol-ended thiophene molecule derivatives; means less reactivity. This molecule with the largest addition energy in comparison with the others is the most possible candidate for MSET application with a good performance.

Among the four boron impurity orientations, the molecule (IV) has the minimum addition energy value. The thiol-ended thiophene has an intermediate addition energy without any boron impurity. As a consequence, both increased and decreased addition energies were calculated due to the number and orientation of the boron impurity in the thiol-ended thiophene molecule. The results obtained in this study will provide further motivation for researchers interested in the conductance dependence of thiol-ended thiophene molecule SET in terms of gate and source/drain bias.

## References

1. Anu, A. Srivastava and M. S. Khan, *Org. Electron Physics, Mater Appl.*, 2018, **53**, 227.
2. A. Nasri, A. Boubaker, B. Hafsi, W. Khaldi and A. Kalboussi, *Org. Electron Physics, Mater. Appl.*, 2017, **48**, 7.
3. M. Liang, J. Yin, K. Chaitanya and X.-H. Ju, *J. Theor. Comput. Chem.*, 2016, **15(3)**, 1650027.
4. A. Srivastava, K. Kaur, R. Sharma, P. Chauhan, U. S. Sharma and C. Pathak, *J. Electron Mater.*, 2014, **43(9)**, 3449.
5. K. Stokbro, *J. Phys. Chem. C*, 2010, 20461.
6. S. Jalili and F. Moradi, *J. Theor. Comput. Chem.*, 2005, **4(4)**, 1001.
7. A. Srivastava, B. Santhibhushan and P. Dobwal, *Int. J. Nanosci.*, 2013, **12(6)**, 1.

Çapanlar *et al.*: The influence of boron impurity for the adiabatic charging energies of thiol-ended thiophene *etc.*

8. E. Von Grotthuss, A. John, T. Kaese and M. Wagner, *Asian J. Org. Chem.*, 2018, **7(1)**, 37.
9. M. Velinova, V. Georgiev, T. Todorova, G. Madjarova, A. Ivanova and A. Tadjer, *J. Mol. Struct. THEOCHEM.*, 2010, **955(1-3)**, 97.
10. A. Srivastava, B. Santhibhushan and P. Dobwal, *Appl. Nanosci.*, 2013, **2**, 1.
11. B. Santhibhushan, M. S. Khan, A. Srivastava and M. S. Khan, *IEEE Trans. Electron Devices*, 2016, **63(3)**, 1232.
12. A. Srivastava, B. Santhibhushan, V. Sharma *et al.*, *J. Electron Mater.*, 2016, **45(4)**, 2233.
13. Anu, A. Sharma, M. S. Khan, A. Srivastava, M. Husain, M. S. Khan, *IEEE Trans. Electron Devices*, 2017, **64(11)**, 4628.
14. J. L. Bredas, J. P. Calbert, DA. da Silva Filho and J. Cornil, *Proc. Natl. Acad. Sci.*, 2002, **99(9)**, 5804.
15. S. J. Ray and R. Chowdhury, *J. Appl. Phys.*, 2014, **116(3)**.
16. M. W. Schmidt, K. K. Baldrige, J. A. Boatz *et al.*, *J. Comput. Chem.*, 1993, **14(11)**, 1347.
17. A. D. Becke, *Phys. Rev. A*, 1988, **38(6)**, 3098.
18. C. Lee, W. Yang and R. G. Parr, *Phys. Rev. B*, 1988, **37(2)**, 785.
19. J. J. Engelberts, R. W. A. Havenith, J. H. Van Lenthe, L. W. Jenneskens and P. W. Fowler, *Inorg. Chem.*, 2005, **44(15)**, 5266.
20. J. C. Santos, W. Tiznado, R. Contreras and P. Fuentealba, *J. Chem. Phys.*, 2004, **120(4)**, 1670.
21. J. C. Santos, J. Andres, A. Aizman and P. Fuentealba, *J. Chem. Theory. Comput.*, 2005, **1(1)**, 83.
22. M. D. Hanwell, D. E. Curtis, D. C. Lonie, T. Vandermeersch, E. Zurek and G. R. Hutchison, *J. Cheminform.*, 2012, **4(1)**, 17.
23. C. Allgood, Y. Lin, Y. C. Ma and B. Munson, *Org. Mass Spectrom.*, 1990, **25(10)**, 497.
24. R. S. Ruoff, K. M. Kadish, P. Boulas and E. C. M. Chen, *J. Phys. Chem.*, 1995, **99(21)**, 8843.
25. K. K. Likharev, *Proc. IEEE*, 1999, **87(4)**, 606.
26. Anurag, B. S. Srivastava and P. Dobwal, *Int. J. Nanosci.*, 2013, **12(6)**, 1.

